CAPTURING NETS FOR ACTIVE DEBRIS REMOVAL: A FOLLOW-UP ON MICROGRAVITY EXPERIMENT DESIGN TO VALIDATE FLEXIBLE DYNAMIC MODELS

Medina, A. [(1)], Cercós, L. [(1)], Stefanescu, R. [(2)],
Benvenuto, R. [(3)], Lavagna, M. [(3)], González, I. [(4)], Rodríguez, N. [(4)], Wormnes, K. [(5)]

[(1)] GMV, Isaac Newton 11, 28760 Tres Cantos, Spain, amedina@gmv.com, lcercos@gmv.com,
[(2)] GMV-Romania, Calea Victoriei 145, 010072 Bucharest, Romania, rmstefanescu@gmv.com,
[(3)] Politecnico di Milano, Via La Masa 34, 20156 Milano, Italy, riccardo.benvenuto@polimi.it, michelle.lavagna@polimi.it
[(4)] PRODINTEC Technology Centre, Avda. Jardín Botánico 1345, 33203 Gijón, Spain, ige@prodintec.com, nrl@prodintec.com
[(5)] ESA/ESTEC, Keplerlaan 1, 2200 AG Noordwijk – The Netherlands, kjetil.wormnes@esa.int

ABSTRACT

As space debris is recognized as a major risk for space missions the European Space Agency (ESA) through the Clean Space Initiative is funding several activities to mitigate this risk. The ESA-funded PATENDER activity (Net parametric characterization and parabolic flight) has a clear objective of developing a confident mean to further investigate, develop and validate the concept of using nets for actively removing space debris of different characteristics.
A net simulator will be validated in a parabolic flight experiment where microgravity conditions can be reached during some few tens of seconds. A set of nets with masses attached at the corners will be launched using a pneumatic-based dedicated mechanism in order to simulate the capture of large space debris. High-speed motion cameras will record the experiment to perform afterwards the reconstruction of the net trajectory including the wrapping around a satellite mock-up target.

1. INTRODUCTION TO ADR USING NETS

Nowadays Active Debris Removal (ADR) techniques appears as solution to mitigate effects of the space debris (6000 satellites in orbit and only 900 in an operational state, 16.000 objects tracked by US Space Surveillance Network, 200 on-orbit fragmentations since 1961, 700.000 objects larger than 1cm; 4 recorded examples of collisions). The space debris problem could be even worst in the near future as almost 1200 new satellites are expected to be launched in the next 8 years (Euroconsult forecast).
Today there is a great concern and consensus that collisions could become the main future source for new debris objects, possibly leading the space debris environment into a chain reaction, rendering some orbital regions with an unacceptably risk for operations. Since the first awareness of the problem in the early 1960s, the global dimension of this problem has been understood today.
ESA, with its Clean Space initiative focuses its efforts in four different branches: 1) Eco-design, 2) Green technologies, 3) Space debris mitigation and 4) Space debris remediation. Within the approach of space debris remediation there exists two different approaches: a) using robotics arms and b) using throw-nets.
The use of throw-nets seems particularly promising for capturing objects in space in cases where robot grasping will be difficult [1][2] (targets may have unpredictable spins and no suitable grasping points). Throw-net approach presents simplifications with respect to other technologies because of the less stringent robotics needed and complexities. Moreover, the distance at which the chaser can operate from the debris can bring some simplifications to the safety of the debris removal operations, which can be particularly important for big non-passivated debris.
The throw-net technique brings however, some critic points that have to be carefully considered, both for the development of the technologies and for the mission realization. For instance, angular motion synchronization of the chaser with respect to the debris may still be needed. In addition, and most importantly, the non-rigid dynamics of the tether and net deployment, capture and closure must be carefully assessed as they impose new challenges both in terms of GNC design and development and in the overall mission operations.
In order to support the net design a dynamics simulator has been proved to be necessary. The net dynamics simulator has the aim of reproducing the behaviour and the effects of capturing space debris using different configurations in terms of net shape and dimensions. It can faithfully reproduce the net dynamics during the following phases: launching, deployment, target wrapping and deorbiting manoeuvres. The PATENDER simulator [3] is going to be validated within a Novespace parabolic flight (June 2015) where microgravity conditions can be reached during almost 20 seconds. The aim is to reconstruct the trajectory of net knots and bullets over time during deployment and

mock-up wrapping in order to validate the numerical simulator. The parabolic flight experiment will also raise the technology readiness level (TRL) of space throw-net techniques to TRL 5/6 (representative prototype tested in a relevant environment).

2. EXPERIMENT DESIGN

The net design is the key feature of such a system: it must be appropriately light, strong and elastic. In particular, its elasticity strongly influences the overall dynamics behaviour. Candidate materials have been identified in HM-HT (high modulus-high tenacity) synthetic fibres, mainly aramid (as Kevlar or Technora) and HMPE (as Dyneema). Technora has been chosen as baseline for the net model validation experiment, after trading-off candidate materials based on the following criteria:

- Technora properties (space qualified, high tensile strength, high impact strength, fatigue resistance, dimensional stability, heat resistance, chemical resistance), not necessarily related to the experiment but to the operative conditions;
- Experiment requirements (colour coding, manufacturing and assembly, representativeness and dynamic scaling).

The representativeness is guaranteed by scaling the net both geometrically and dynamically, while keeping the same material. Net diameters and mesh size have been selected according to this latest point and to experiment requirement (knot size on pixel size ratio). All nets have been selected to be quadrangular with quadrangular mesh to meet experiment requirements both from the reconstruction and validation point of view. Different net sizes and meshes have been selected as reported in Table 1:

Table 1. Characteristics of experimental nets.

Nets	Diameter [mm]	Mesh [mm]	Size [mm]	Mass [grams]
Net 1-A	1	50	900	38
Net 1-B		25	900	73
Net 2-A		50	600	18
Net 2-B		25	600	33

These nets represents a scale 1:40 of the reference scenario (the mock-up satellite is also scaled down to 1:40): therefore they respectively represents a 36 m and a 24 m planar nets.

To fully characterize the Technora ropes' mechanical properties, including damping, tensile tests and dynamical-mechanical tests have been conducted at Politecnico di Milano laboratories. These tests allowed to reduce the number of uncertain parameters in the flexible dynamics model validation process.

Tensile tests have run both on braids and knotted braids, as visible in Figure 1 dynamical tests have run both on DMA analyser and rotational rehometer, visible in Figure 2. Material tests have allowed to estimate ropes axial bending and torsional stiffness and damping, as well as breaking strength and strain (including knots' strength reduction). Results are summarized in Table ***2***.

Figure 1. Tensile tests on Technora single braids and knotted braids

Figure 2. Dynamical tests on DMA analyser and rotational rehometer.

Table 2. Material tests' results.

Young's modulus [GPa]	25.367
Breaking stress [GPa]	1.626
Breaking strain [%]	6.43
Knot breaking stress [GPa]	0.536
Axial stiffness per unit length [N]	9.84·103
Torsional stiffness per unit length [Nm2]	2.94·10-6
Bending stiffness per unit length [Nm2]	1.34·10-6
Axial damping ratio [-]	0.106
Torsional damping ratio [-]	0.079
Bending damping ratio [-]	0.014

The parabolic flight experiment has also been designed to maximize the chances of wrapping success, by tuning net shooting velocity/angle and target position.

The net deployment has been extensively simulated using the acceleration profiles provided by Novespace to evaluate net trajectory, also including Coriolis and centrifugal accelerations as well as air drag.

As outcome of simulations, it was possible to conclude that if the net is shot at a velocity below 1 m/s, the trajectory will be completely random because it will mainly depend on the residual acceleration profile during deployment, as visible in Figure 3, where two unsuccessful wrapping simulations are presented.

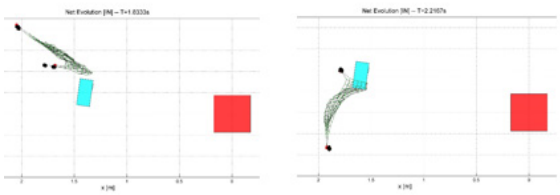

Figure 3. Two different net simulations with unsuccessful wrappings.

A first mitigating, but not decisive, action has been to shoot the net with a delay after parabola injection, to exploit the central part of the parabola where microgravity is supposed to be better. This is also consistent with the analysis of different accelerations' orders of magnitude acting on the net, as reported in the Tab. 3 (the reference system is X-axis = roll axis toward the cockpit, Y-axis = pitch axis towards left wing looking at the cockpit, Z-axis = yaw axis):

Table 3: Acting accelerations during net deployment – orders of magnitude and direction

ACCELERATION	MAXIMUM VALUES	AXIS
Disturbance [m/s^2]	≈ ±0.5	Z axis
Coriolis [m/s^2]	≈ +0.06	Z axis
Centrifugal [m/s^2]	≈ ±0.005	X axis
Air drag [m/s^2]	≈ 10^-6 ÷10^-7	- V axis

A calibrated IMU will be synchronized with the system during microgravity tests to record acceleration profiles, as another key feature for the posterior model validation. In order to increase the chance of the net hitting the target, a compromise between the following degrees of freedom have proved to be effective:

- to shoot the net at increased velocity (to make it go straight) up to a certain limit, due to cameras frame rate/shutter speed, scaling/representativeness and air drag;
- to approach the target towards the canister, while guaranteeing the net complete deployment and cameras field of view coverage.

For example, Figure 4 shows that the target is placed at 1.3 m from the shooting system and the bullets are shot at 1.2 m/s with a divergence angle of 21°, which correspond to a centre of mass velocity of ≈ 1 m/s.

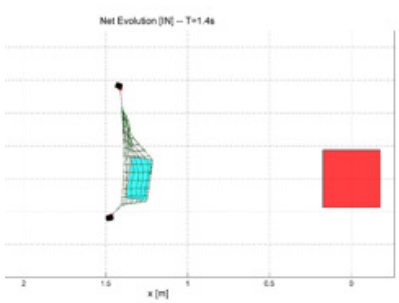

Figure 4. Net simulation with successful wrapping.

3. NET DYNAMICS SOFTWARE SIMULATOR

The PATENDER Simulator has the aim of reproducing the behaviour and the effects of capturing space debris using different Net configurations. The visualization of the net deployment is realized using Blender as a graphic interface and Python as a script environment. Blender is one of the most popular Open Source 3D graphics applications in the world. It provides a broad spectrum of modelling, texturing, lighting, animation and video post-processing functionality in one package.

The PATENDER Simulator has the capability of creating, moving and recording the Net evolvement. While the selection of the Net configuration parameters is done through Python script in Blender, the dynamics of the net (orbital dynamics, net deployment and target wrapping) is performed by an external application interfaced through UDP communications channels with two standalone applications:

- Net Pre-processing: It is in charge of generating all arrays of simulation vectors needed for a faster computation of the viscoelastic models. It receives a set of basic input parameters and it generates the initial Propagation Parameters needed to compute the deployment of the net.
- Forward Dynamics Propagator: It is in charge of computing the systematic simulation of the net deployment through the corresponding viscoelastic models. It also includes the wrapping phase using the Bullet Physics library for collision detection with the target satellite and dedicated computation of collision forces.

The creation of the net elements refers to the generation of knots, nodes and bullets using Blender 3D objects. This creation process is performed under the Blender environment using different components and each component being created individual. A net is a mesh of knots composed by the following elements:

- Knots: Intersecting threads with ability to hold specific mass (depending in the manufacturing technology: weaved/knotted)
- Links: Any thread between two knots. It is defined from start to end knots: knot base and knot follower. A link is subdivided into nodes and elements (lumped masses discretizing the thread mass).
- Bullets: Massive elements in charge of deploying the net. Modelled as a rigid body (position and pose).
- Tether(s): managed as additional link(s), defining connection topology between net and chaser.
- Closing Links: managed as additional links. Its length is controlled externally through user inputs.

Flexible elements are mathematically modelled using lumped parameters methods, that have already been employed and validated for underwater flexible structures and fishing nets applications [4].

Next Figure 5 presents an example of a fully-deployed

net of 17x17 knots. The four bullets are displayed in blue while the knots are in red. The links are divided in two nodes and three elements and are displayed as cylinders. Under a Blender integrated interface the user can modify the net characteristics and the visualization viewpoint.

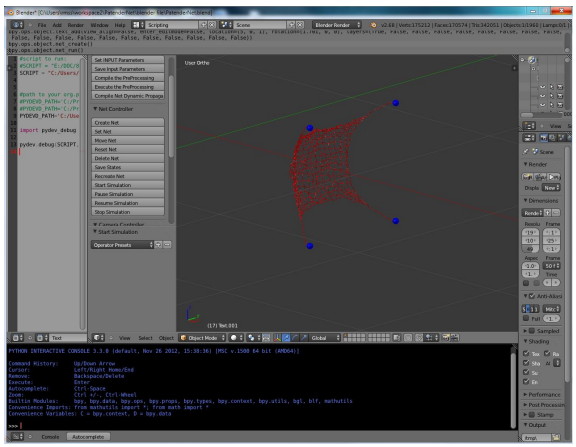

Figure 5. PATENDER 3D visualisation environment.

In order to properly compute the collisions between net and target, our simulator integrates the Bullet collision engine. Bullet is mainly optimized for video-games development with the intention to reproduce coarsely real motion dynamics. For this reason, the Patender Simulator only integrates the Bullet's collision detection, discarding Bullet's contact dynamics. Contact dynamics is implemented based on Hippmann [5] algorithms.

Within the Bullet world the net is represented as a set of cylinders instead of another primitive simpler objects such as spheres allowing to increase the accuracy of the collision; collisions between adjacent cylinders are discarded. However, net dynamics and collision dynamic algorithms considers the net as a set of particles. For this reason, interface equations between both worlds are needed. Figure 6 shows a diagram for contact and dynamics worlds, as well as the interface equations between particles state and cylinders state.

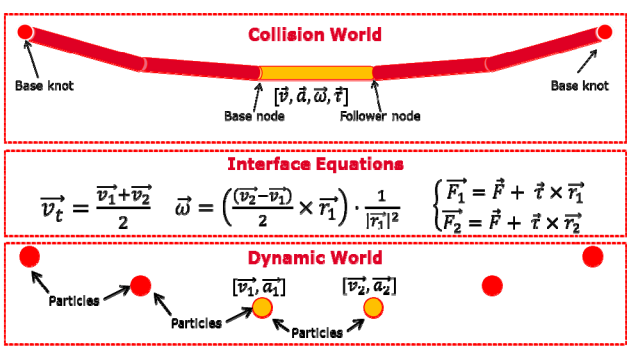

Figure 6. Collision & Dynamic worlds.

4. PARABOLIC FLIGHT SETUP

4.1. Novespace parabolic flight

The PATENDER experiment will be validated by June 9th 2015 in the Novespace 116th parabolic flight campaign (62nd ESA Parabolic Flight campaign) on-board of an Airbus A310 ZERO-G aircraft.

A typical Novespace parabolic flight is composed of 31 parabolas in a roller-coaster mode where six series of 5 parabolas are concatenated with short breaks of 1 minute and 45 seconds between them. After each set of parabolas a long break of 5 to 8 minutes allow to perform minor adjustments of the experiment.

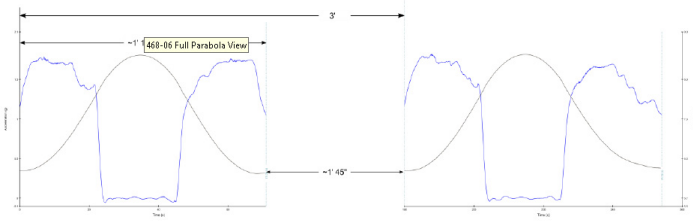

Figure 7. Novespace parabola profile.

Parabolic flights do not represent a public air transportation activity and it does not follow typical certification process of Airworthiness (CoA). Instead of that Novespace manages the flight according to internal security procedures. The PATENDER experiment has followed a strict certification process to determine and accommodate safety rules established by Novespace. A Experiment Safety Data Package has been elaborated together with Novespace enabling the execution of the PATENDER experiment (see Figure 8) on-board the Novespace aircraft.

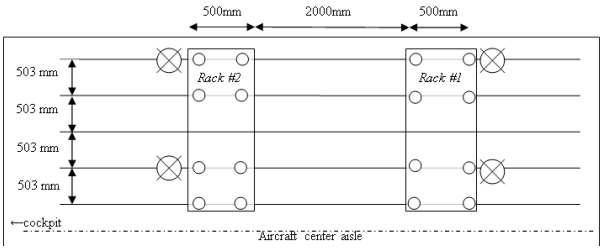

Figure 8. PATENDER experiment location over Novespace Airbus A310 aircraft.

The design, fabrication and assembly of the structures, as well as attachment of the equipment onto the structures, has being carried out under the supervision of Novespace mechanical experts. Maximum allowable loads have been defined to make sure that the structure will sustain an emergency landing.

Rigorous procedures for ground and in-flight operations (as shown by Table 3) have been identified allowing to determine the required number of operators and to identify the role executed by each one.

Table 3. Example of in-flight procedure.

IN FLIGHT PROCEDURE – DURING 8-MINUTE BREAKS		
Task	*Description*	*Operator #*
1	Calibration of cameras set-up using double chessboard.	1
2	Adjustment of bullet liners angle.	2
3	Adjustment of satellite mockup position and orientation.	3
4	Review of cameras and recorders.	1
5	Adjustment of launching pressure.	4

Finally the PATENDER experiment has been evaluated from the point of view of hazard risks grouped into the following categories: fire, electrical shock, structural failure, contamination, collision, injury/illness, explosion/implosion and any other. The following major hazard risks have been identified and appropriate hazard controls and verification methods have been proposed:

- Contact of operators with voltages above 32V.
- Experimenter gets hit or injured by the net/masses.

4.2. Experiment Set-up

During the experiment under micro-gravity conditions, the net launching system will enable to carry out net launching operations. The structure of net launching system is based on a metallic table composed of two parts. The first one is a support table to accommodate all other elements. The second one is a turning plate whose purpose is enabling angular placement of the motherboard to ease the direction of the net launching throughout experiment. This turning plate includes two hinges, a key and a cog and it allows 180º rotations (by increments of 15º). Over such turning plate it is placed a motherboard where the rest of the elements are integrated. These elements are: four bullets, four bullets liners, four angle-adjusting mechanisms and a net container support. Besides, it includes a structure made of aluminium profiles (metallic joint) in order to fix the storage tank, the support table and an electrical connections box.

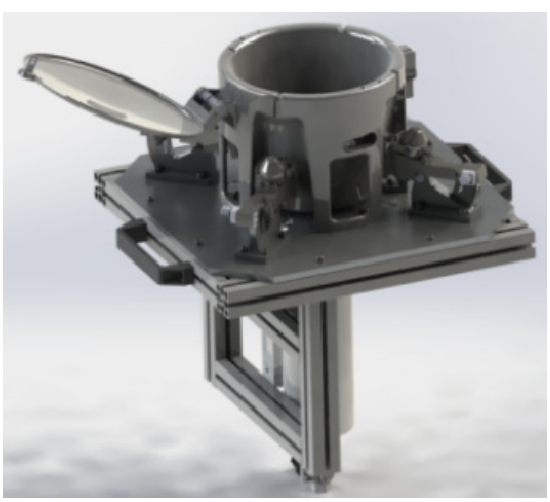

Figure 9. Motherboard with integrated elements.

The mechanism to adjust the launching angle of the bullets can be operated independently for each bullet. It allows an angle range from 15º to 45º, measured from the vertical line / axis. Bullet liners are the mechanical guidelines where bullets are placed. Through these liners, the pressurized air flows out inducing the ejection of the bullets and consequently of the attached net. Bullets design criteria are the geometry, mass, centre of gravity. These design criteria allow bullets to be pushed away over the bullet liner by means of pressurized air. The contact point between the air flow and the bullet must be located under its centre of gravity in order to ensure a longitudinal motion. The pressurized air flow is activated by electrical/pneumatic system.

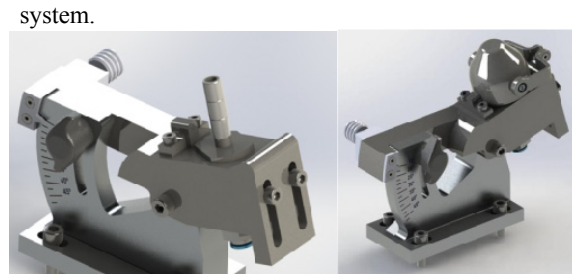

Figure 10. Adjustment mechanism of bullet angles.

Canister or net packing container is the element where the packet net will be placed. Additionally, this canister will be placed inside its support by an adjustment system. The canister is placed in the support and its position is fixed thanks to lateral jugs and magnets. This approach allows placing several types of containers depending on geometry requirements of the net.

The net launching system includes a cover over the canister and its corresponding opening system. The cover is integrated in the container support and it is articulated without interfering with the ejection of the bullets. This articulation is made of a set of antifriction bearing bushes to permit an easier turning. The cover is opened due to the force of two torsion magnets (torsion springs). This force is constant until the locking system of the cover is opened. The cover opening is triggered by a dedicated delayed relay of the electrical system.

The pneumatic system allows to provide pressurized air to launch the bullets at desired initial velocity and angle. It is controlled by an electrical system (see Figure 12) composed by several relays and activated externally by a remote control in the hands of the operator.

The feeding air flow is under air pressure and it goes through a filter to be ready to go to the manometer. After going through the manometer, the pressured air flow is under desired pressure within selected pressure range. Then, the air flow is directed to the V5 valve to fill the air tank as shown by Figure 11. Afterwards, when the bullets launching is carried out, the pressurized air flow goes through valve V4 and it is divided into four lines to reach the four bullets. After activation of V4 valve the bullets are pulled by means of the pressurized air through bullets liners.

Next Figure 11 shows the pneumatic scheme of the net launching system while Figure 12 shows its corresponding electrical diagram.

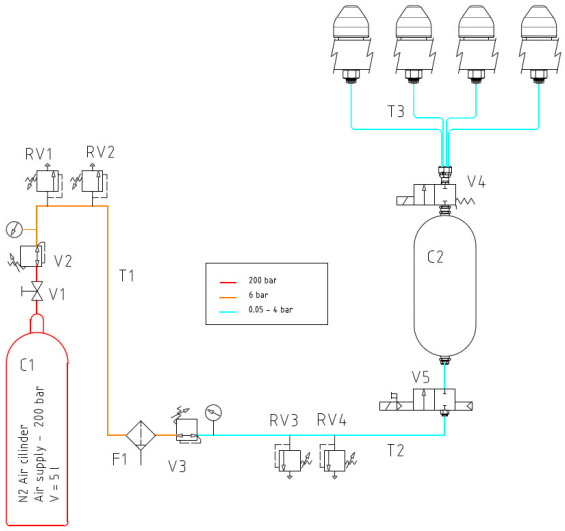

Figure 11. Pneumatic scheme.

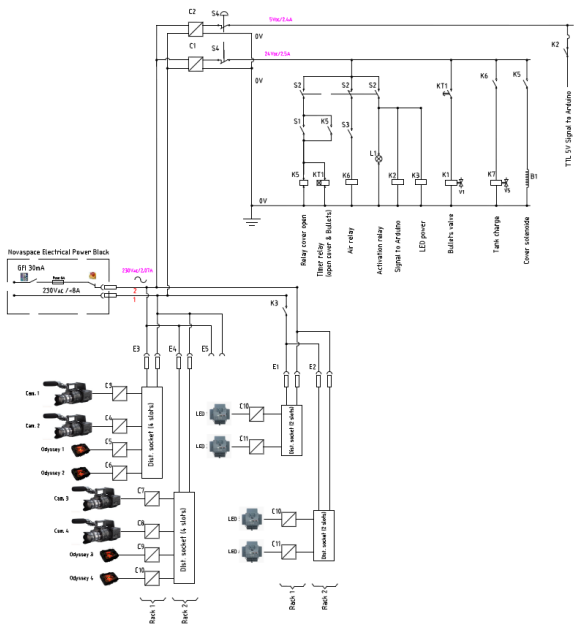

Figure 12. Electrical scheme.

Due to the timing constraints imposed by the parabolic flight characteristics, the net container has been designed as an independent element from net launching system. As result, a reload or charge/discharge tool has been designed to ease operator tasks and optimize the time between parabolas. This reload tool (see Figure 13) allows an easy assembly of bullets and net into the canister.

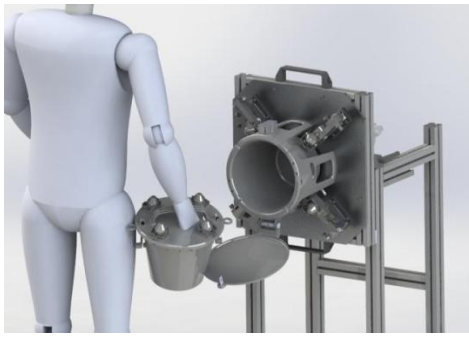

Figure 13. Operating handling the net reload tool.

The PATENDER experiment will be performed in an aircraft requiring a specific set-up adapted to the parabolic flight requirements. As result, the set of elements required is composed of two racks where elements are placed (Figure 14): rack #1 on the right and rack #2 on the left.

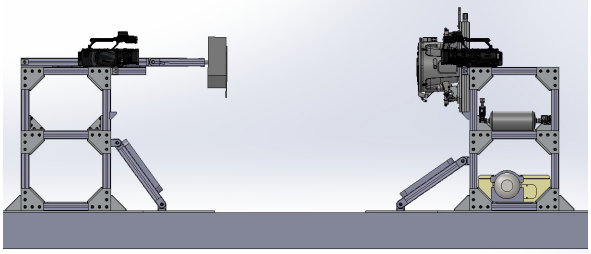

Figure 14. Parabolic flight set-up based in two racks.

The rack #1 as shown by Figure 15 is mainly composed of a metallic structure where the required elements are placed: two cameras, LED plates and the net launching system including separately an air tank, an electronic box (in yellow) and the pneumatic system (in grey). The two cameras are placed on the top corners of the structure separated a distance of two meters. Between them, it is placed the net launching system. At its back it is positioned the air tank. The electronic box and the pneumatic system are situated in the bottom of the rack and connected to the rest of component of net launching system. Finally two LED lamps are placed on the bottom of the structure and the whole rack is fixed to the floor using four screwed plates.

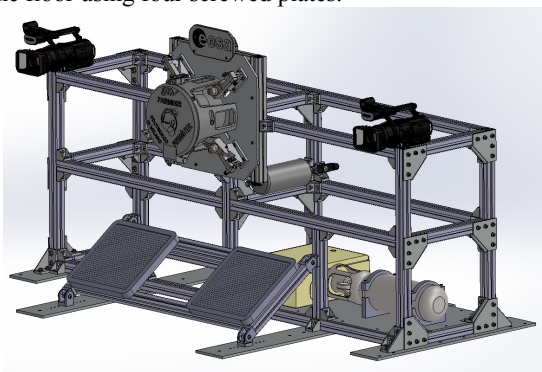

Figure 15. Rack #1 structure.

Next Figure 16 shows the rack #2 configuration whose main metallic structure integrates required elements such as cameras, LED plates and the satellite mock-up. On the top of the structure, the two cameras are placed at a distance between them of 2 meters. In the middle of them, a structural arm supports the mock-up. This arm can be extended up to 300 mm and it can be turned within angle range [-90º-90º]. At the bottom of the rack structure two LED lamps are placed to illuminate the overall scenario while the experiment is recorded.

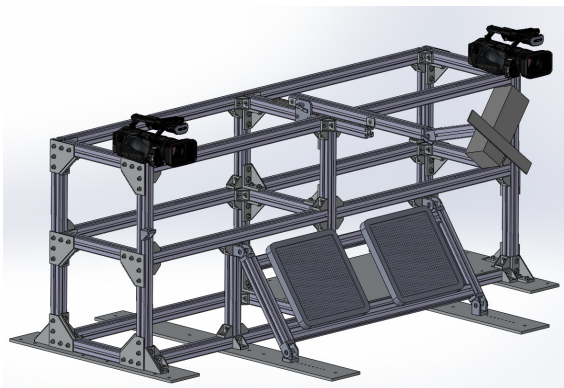

Figure 16. Rack #2 structure.

4.3. 3D Reconstruction

Four Sony Nex-FS700RH cameras will record the experiment at 60 fps in 4K resolution, in order to allow the 3D reconstruction of the deployment and wrapping around the target. Such high resolution is due to the requirement on the ratio between net knots size on pixel size, which must be ≥ 5/6, to guarantee knots extraction robustness. An increased shutter speed has been selected to minimize the motion blurring effects while preserving a sufficient luminosity of the image.

The cameras are placed as far as possible from each other to increase both the baseline (reconstruction accuracy) and the envelope that their field of view can cover with an acceptable resolution for reconstruction.

The cameras are placed in landscape configuration on top of the racks for stability purposes (e.g. to minimize their vibrations) and rotated around Z-axis of 45° and 35° for the front stereo-couple and the rear pair respectively. The focal length is set to 14 to reach the needed field of view; however such a wide angle requires finer calibration, especially at boundaries, to minimize distortions. The iris aperture and focus are finally tuned to allow the correct depth of field.

Next Figure 17 shows the field of views and stereo couple coverage for both the front and rear pairs. Setting up a synthetic environment as the one presented in Figure 17 and Figure 18, has proven to be useful allowing a finer tuning of camera setting in the experimental set-up.

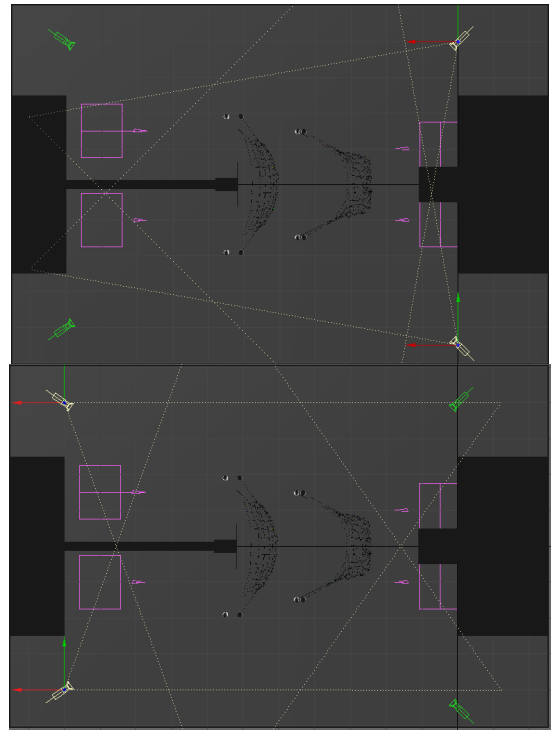

Figure 17. Fields of view and stereo coverage – front and rear stereo pair of cameras.

Figure 18 presents a simulated net view for one front and one rear camera.

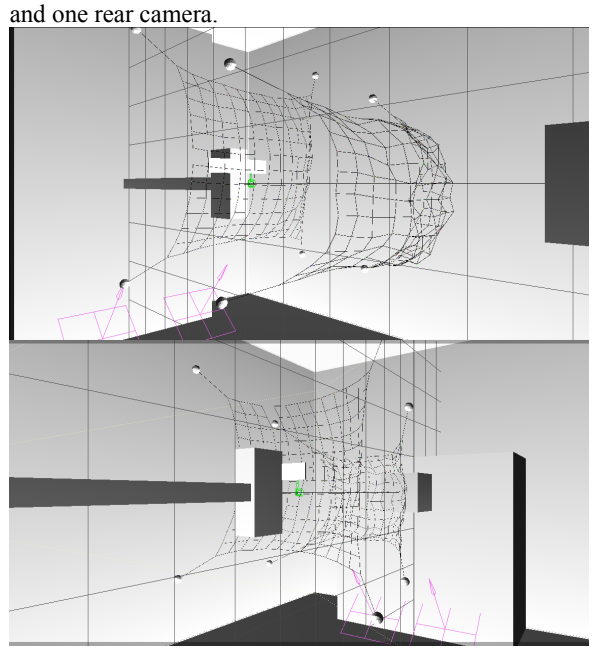

Figure 18. Net simulated deployment – front and rear views.

Net knots have been colour-coded with fluorescent pigments, as depicted by Figure 19, and their 3D trajectory reconstruction procedure is based on the image processing for colour segmentation, stereo matching of the segmented knot and iterative closest

point (ICP) for time tracking of knots, as described in [6]. For all these reasons a uniform background is necessary as well as proper illumination: a LED-based illumination system to be placed on the floor has been selected meeting parabolic flight safety constraints (heat, luminosity, operations, failures) and lighting conditions requirements, which are very demanding with the needed resolution, frame rate and shutter speed.
An example of colour segmentation and knots localization is presented in Fig. 10: the first image is the result of raw file processing for white balance and gain correction, the second is the yellow filter and the third is the final binary image exploited by the reconstruction algorithm.

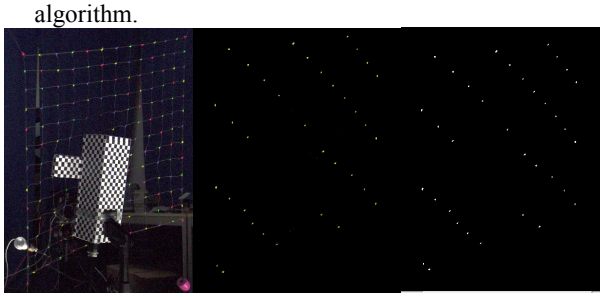

Figure 19. Colour segmentation of yellow knots: processed image from raw, yellow filtering and final binary image.

The topology is reconstructed when the net is completely deployed, and a univocal identifier is attributed to every knot. Then the tracking step is performed backwards and forwards for every knot until they become occluded from both the stereo pairs. The tracking step also allows to increase the accuracy of the 3D reconstruction by using as constraints that between two consecutive frames every knot should occupy the closest allowed position with respect to the previous frame and that the maximum distance between knots cannot be greater than the mesh size.
Finally a partial wrapping reconstruction performed on ground is presented in Figure 20. Reconstruction accuracy decreases for the knots that are only seen by one of the cameras. If the other camera pair can simultaneously localize the occluded knots, the error can be corrected; otherwise the knot position is marked as estimated instead of reconstructed.

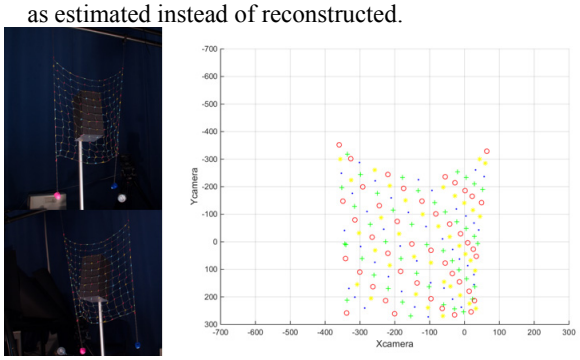

Figure 20. Ground test: reconstruction of partially wrapped net.

5. CONCLUSIONS

The PATENDER simulator will be validated in the Novespace parabolic flight experiment where microgravity conditions can be reached during some few tens of seconds. Several nets will be launched using a pneumatic-based dedicated mechanism in order to represent the capture of large space debris.
The parabolic flight experiment has been designed to maximize the probability of wrapping success, by tuning net shooting velocity/angle and target position.
The launching mechanism is composed by a motherboard supporting these elements: a net container and four adjustable bullets liners and a pneumatic system managing an air tank and several latching valves. The operator places the net within the container and the corner masses over the bullets liners and fills the air tank with pressurized air. At this stage the net is ready to be launched at the desired initial velocity.
High-speed motion cameras will record the experiment in order to allow the 3D reconstruction of the deployment and wrapping around the target phases and the validation of the software simulator. Net knots have been colour-coded and their 3D trajectory reconstruction procedure is based on the image processing for colour segmentation, stereo matching of the segmented knot and iterative closest point (ICP) for time tracking of knots. Vision algorithms from Politecnico di Milano have been adapted for the specific features of this experiment and successfully tested on real acquisitions on ground. The acquisition set-up has been designed in order to reduce the occlusions due to the target mock-up and to maximize the stereo field-of-view to increase the visibility window.
The output of this activity will be the implementation of a high-fidelity throw-net simulator validated through a parabolic flight campaign.

6. REFERENCES

[1] "*Robotic Geostationary Orbit Restorer*", GSP phase A final report, Astrium SI, Bremen, June 2003. Doc no: ROG-SIBRE-FP.

[2] Wormnes, K. et.al. "*Throw-nets and tethers for robust space debris capture"*, In IAC2013, Beijing, October 2013.

[3] Cercós, L. et.al. "*Validation of a Net Active Debris Removal simulator within parabolic flight experiment"*, i-SAIRAS 2014, Montreal, June 2014.

[4] C. Lee, B. Cha, and H. Kim, "*Physical modeling for underwater flexible systems dynamic simulation*", Ocean Engineering, pages 331-347, October 2005.

[5] Hippmann, G. "*An algorithm for compliant contact between complexly shaped surfaces in multibody dynamics*". IDMEC/IST, Lisbon, Portugal, July 1-4, 2003).

[6] "*Visual 3D Modeling from Images*", Pollefeys M. Notes, University of North Carolina, USA.